

The Starburst in the Abell 1835 Cluster Central Galaxy: A Case Study of Galaxy Formation Regulated by an Outburst from a Supermassive Black Hole

B. R. McNamara¹, D. A. Rafferty¹

L. Birzan¹, J. Steiner¹, M. W. Wise³, P. E. J. Nulsen², C. L. Carilli⁴, R. Ryan^{1,5}, M. Sharma¹

ABSTRACT

We present an optical, X-ray, and radio analysis of the starburst in the Abell 1835 cluster's central cD galaxy. The dense gas surrounding the galaxy is radiating X-rays with a luminosity of $\sim 10^{45}$ erg s⁻¹ as its temperature ranges from ~ 9 keV to ~ 2 keV, consistent with a cooling rate of $\sim 1000 - 2000 M_{\odot}$ yr⁻¹. However, Chandra and XMM-Newton observations found less than $200 M_{\odot}$ yr⁻¹ of gas cooling below ~ 2 keV, a level that is consistent with the cD's current star formation rate of $100 - 180 M_{\odot}$ yr⁻¹. One or more heating agents (feedback) must then be replenishing the remaining radiative losses. The heat fluxes from supernova explosions and thermal conduction alone are unable to do so. However, a pair of X-ray cavities from an AGN outburst has deposited $\simeq 1.7 \times 10^{60}$ erg into the surrounding gas over the past 40 Myr. The corresponding jet power $\simeq 1.4 \times 10^{45}$ erg s⁻¹ is enough to offset most of the radiative losses from the cooling gas. The jet power exceeds the radio synchrotron power by ~ 4000 times, making this one of the most radiatively inefficient radio sources known. The large jet power implies that the cD's supermassive black hole accreted at a mean

¹Astrophysical Institute and Department of Physics & Astronomy, Ohio University, Clipping Labs, Athens, OH 45701

²Harvard-Smithsonian Center for Astrophysics, MS 70, 60 Garden Street, Cambridge, MA 02138, and University of Wollongong

³Massachusetts Institute of Technology, Kavli Institute, Cambridge, MA 02139-4307

⁴National Radio Astronomy Observatory, Socorro, NM

⁵Department of Physics & Astronomy, Arizona State University, Tempe, AZ

rate of $\sim 0.3 M_{\odot} \text{ yr}^{-1}$ over the last 40 Myr or so, which is a small fraction of the Eddington accretion rate for a $\sim 10^9 M_{\odot}$ black hole. The ratio of the bulge growth rate through star formation and the black hole growth rate through accretion is consistent with the slope of the (Magorrian) relationship between bulge and central black hole mass in nearby quiescent galaxies. The surface densities of molecular gas and star formation follow the Schmidt-Kennicutt parameterizations, indicating that the high pressure environment does not substantially alter the IMF and other conditions leading to the onset of star formation. The cD in Abell 1835 appears in many respects to be a textbook example of galaxy formation governed by the gravitational binding energy released by accretion onto a supermassive black hole. The consistency between net cooling, heating (feedback), and the cooling sink (star formation) in this system resolves the primary objection to traditional cooling flow models.

Subject headings: clusters of galaxies: general — cooling flows: individual (Abell 1835)– galaxies: active, galaxies: elliptical and lenticular, cD– galaxies: starburst– X-rays: galaxies: clusters

1. Introduction

The most luminous galaxies in the Universe lie at the centers of galaxy clusters. Central dominant galaxies (which we refer to as cD galaxies) have masses of $\sim 10^{13} M_{\odot}$ and halos extending hundreds of kiloparsecs into the surrounding cluster (Sarazin 1986). They are able to grow to such large sizes by swallowing stars and gas from neighboring galaxies (Gallagher & Ostriker 1972, Hausman & Ostriker 1978, Merritt 1985) and by capturing the cooling intracluster gas (Fabian & Nulsen 1977, Cowie & Binney 1977). The bulges of many cD galaxies are currently growing rapidly through gas accretion and star formation proceeding at rates of $\sim 10 - 100 M_{\odot} \text{ yr}^{-1}$ (Johnstone, Fabian, & Nulsen 1987, McNamara & O’Connell 1989, 1993, Crawford et al. 1999, McNamara, Wise, & Murray 2004, Hicks & Mushotzky 2005, Rafferty et al. 2006, this paper). These rates rival or exceed those found in massive galaxies at redshifts in the range $z = 2 - 3$ (Juneau et al. 2005), yet they are found in nearby cooling flow clusters characterized by cuspy X-ray surface brightness profiles and rapidly cooling gas. The starbursts are fueled by $\sim 10^{8-11} M_{\odot}$ reservoirs of cold atomic and molecular gas (Jaffe, Bremer, & Van der Werf 2001, Jaffe, Bremer, & Baker 2005, Donahue et al. 2000, Falcke et al. 1998, Heckman et al. 1989, Voit & Donahue 1997, McNamara, Bregman, & O’Connell 1990, O’Dea, Baum, & Gallimore 1994, Taylor 1996, Jaffe 1990, Edge 2001, Salomé & Combes 2003). Bright optical emission nebulae and X-ray emission

from clumps and filaments of gas at temperatures of $\sim 10^7$ K and densities of $\sim 10^{-2}$ cm^{-3} are a characteristic signature of these systems (McNamara et al. 2000, Fabian et al. 2003, McNamara, Wise, & Murray 2004, Crawford, Sanders, & Fabian 2005, Jaffe, Bremer, & Baker 2005). Under these conditions, the hot gas should cool and condense onto the central galaxy at rates of several hundred to over $1000 M_{\odot} \text{yr}^{-1}$ (Fabian 1994). However, an inflow at this level would overwhelm these galaxies with cold gas and star formation exceeding the observed levels by factors of 10 or more. This implies that the cooling gas is deposited in an invisible form of matter, or that it is condensing out of the intracluster medium at a much lower rate.

Progress on this problem stalled for more than a decade until the Chandra and XMM-Newton observatories revealed that most of the cooling gas is not condensing out of the hot intracluster medium, but rather it is maintained at X-ray temperatures by one or more heating agents. The spectra of cooling flows fail to show the soft X-ray emission lines emerging from gas cooling out of the X-ray band at the expected strength (Molendi & Pizzolato 2001; David et al. 2001, Fabian et al. 2001, Peterson et al. 2001, Peterson et al. 2003, Tamura et al. 2001, Böhringer et al. 2002). Instead, the gas seems to be cooling down to about 1/3 of the average gas temperature at the expected rates, but most of it fails to continue to cool and condense onto the cD galaxy (Peterson et al. 2003). These observations do not, however, exclude cooling below X-ray temperatures at levels that are comparable to the observed star formation rates (McNamara 2004, McNamara, Wise, & Murray 2004, Hicks & Mushotzky 2005, Rafferty et al. 2006). Therefore, while the bulk of the cooling gas remains hot, enough may be condensing onto cD galaxies to drive star formation and to fuel the active nucleus (AGN) at substantial rates.

Potential heating mechanisms include thermal conduction from the hot gas surrounding the cool core (Tucker & Rosner 1983, Bertschinger & Meiksin 1986, Narayan & Medvedev 2001), subcluster mergers (Gomez et al 2002), supernovae (Silk et al. 1986), and AGN outbursts (Tabor & Binney 1993, Binney 2004, Soker et al. 2001, Ciotti & Ostriker 1997), among others. However, the stringent demands on these mechanisms have been met with varying degrees of success. X-ray cooling is persistent, powerful, and widespread. An effective heating mechanism must be able to cope by producing a heat flux of $\sim 10^{44} - 10^{45}$ erg s^{-1} persisting over several Gyr and distributing the heat throughout a cooling volume that is comparable to the full extent of the central galaxy. Supernova explosions are generally too weak and too localized; mergers are powerful enough but cannot be relied upon to provide a persistent source of heat; and conduction proceeds with great difficulty deep in the cool cores of clusters. Recurrent AGN outbursts have emerged as the agent best able to meet these requirements, although thermal conduction still may play a significant role near the cooling radius (cf., Ruszkowski & Begelman 2002, Rosner & Tucker 1989, Narayan & Medvedev

2001, Voigt et al. 2002, Soker, Blanton, & Sarazin 2003, Zakamska & Narayan 2003).

cD galaxies are known to harbor powerful radio sources (Burns 1990). Outbursts from AGN associated with these sources generate cavities, ripples, and shock fronts in the hot gas surrounding them, and the energy dissipated is enough to balance radiative cooling losses in many systems (McNamara et al. 2000, 2001, 2005, Bîrzan et al. 2004, Young et al. 2002, Forman et al. 2005, Nulsen et al. 2002, 2005 a, b, Blanton et al. 2001, Heinz et al. 2002, Kraft et al. 2005, Rafferty et al. 2006, and others). These outbursts generate $\sim 10^{55}$ erg in giant ellipticals and groups (Finoguenov & Jones 2001), to upward of $\sim 10^{61}$ erg in rich clusters (Bîrzan et al. 2004, McNamara et al. 2005, Nulsen et al. 2005 a, b). This is enough energy to quench cooling entirely in isolated ellipticals (Finoguenov & Jones 2002, Best et al. 2006), and to drive outflows and buoyant bubbles that regulate cooling flows (Rafferty et al. 2006). The most powerful outbursts are able to heat the gas beyond the cooling region (McNamara et al. 2005, Nulsen et al. 2005 a, b) and contribute to the overall entropy excess in clusters (Voit & Donahue 2005). The past few years have seen remarkable growth in the number of computer simulations of pressure-confined jets pushing through hot atmospheres. The simulations generally show that much of the jet energy is thermalized and thus is able to heat the gas. However, the important details concerning how and how much of the jet energy is thermalized and distributed throughout the cooling region, and how the cavities are stabilized are not entirely understood (e.g., Reynolds, Heinz, & Begelman 2002, Basson & Alexander 2002, Kaiser & Binney 2003, Brüggen & Kaiser 2001, 2002 Brüggen 2003, Soker et al. 2001, Brighenti & Mathews 2002, Churazov et al. 2001, Churazov et al. 2002, Quilis et al. 2001, De Young 2003, Jones & De Young 2004, Omma et al. 2004, Ruszkowski, Brüggen, & Begelman 2004, Vernaleo & Reynolds 2005, Piffaretti & Kaastra, 2006, and many others).

These issues are deeply rooted in the more general problem of galaxy formation. In the standard cold dark matter hierarchy (White and Rees 1978), small halos merge into larger ones while the captured baryons cool and condense onto the progenitors of mature galaxies, a process that should still be occurring in clusters today (Cole 1991, Blanchard, Valls-Gabaud, & Mamon 1992, Sijacki & Springel 2005). This paradigm successfully describes the distribution of matter on large scales. However, it has difficulty dealing with the fact that even the biggest galaxies seemed to have formed quickly. Furthermore, CDM models that include gravity alone over-predict the fraction of cold baryons (Balogh et al. 2001), and thus they predict bigger galaxies and more of them than are observed (Voit 2005). The jumbo cD galaxies are a case in point. Although they have grown to enormous sizes, they should have absorbed more of the cooling baryons in clusters and grown larger still (Sijacki & Springel 2005). Instead of condensing onto the cD, most of the baryons in clusters reside today in the hot gas between the galaxies. The work-around involves nongravitational heating by early supernova explosions and AGN. Supernova explosions are surely important at some level, and

they are essential for enriching the gas with metals (Metzler & Evrard 1994, Borgani et al. 2002, Voit 2005). But they are generally too feeble and localized to truncate star formation in massive galaxies (Borgani et al. 2002). Furthermore, in the closely related “preheating” problem, they have difficulty boosting the entropy level of the hot gas to the observed levels, particularly in cooler clusters (Wu et al. 2000, Voit & Donahue 2005, Donahue et al. 2005).

A great deal of progress on these problems has been made in recent work showing that powerful AGN outbursts in cD galaxies can supply enough energy to reduce or quench cooling flows and thus regulate the growth of massive galaxies (e.g., Bîrzan et al. 2004 and references therein). At the same time, lower limits on the outburst energies, which can now be measured reliably using X-ray cavity and shock properties imply that the supermassive black holes powering them are growing at typical rates of $\sim 10^{-3} M_{\odot} \text{ yr}^{-1}$ (Rafferty et al. 2006). In some cases the growth rates are approaching or modestly exceed $\sim 1 M_{\odot} \text{ yr}^{-1}$ (McNamara et al. 2005, Nulsen et al. 2005 a, b) rivaling those during the most rapid periods of black hole growth in the early Universe. Except in the most powerful outbursts, they accrete at a small fraction of the Eddington rate (Rafferty et al. 2006), through a combination of cold disk accretion and Bondi-Hoyle accretion of the hot gas surrounding them (Rafferty et al. 2006). Bondi-Hoyle accretion is not required as there is an adequate supply of cold fuel in cDs to accommodate extended periods of rapid accretion.

Supermassive black holes may reside at the centers of most if not all massive bulges, and thus they appear to be an inevitable consequence of galaxy formation (Kormendy and Richstone 1995). The well-known correlations between bulge luminosity, velocity dispersion, and central black hole mass (Gebhardt et al. 2000, Ferrarese & Merritt 2000) show that the growth of galaxies and supermassive black holes are closely connected, perhaps in part through the regulation of inflowing gas by AGN outbursts (Begelman et al. 2005, Springel, Di Matteo & Hernquist 2005). Cooling flows have emerged among the few places in the nearby Universe where bulge and supermassive black hole growth in massive galaxies can be examined in quantitative detail. The conditions there serve as a testbed for feedback-driven galaxy formation and non gravitational heating models (Sijacki & Springel 2006).

We examine these issues using deep U and R images of the central region of the $z = 0.252$ cluster Abell 1835, we compare them to new and archival Chandra images, and we examine the relationships between cooling and star formation in the cD galaxy. Throughout this paper, we assume $H_0 = 70 \text{ km s}^{-1} \text{ Mpc}^{-1}$, $\Omega_m = 0.3$, $\Omega_{\Lambda} = 0.7$, $z = 0.2523$, a luminosity distance of 1274 Mpc, and a conversion between angular and linear distance of 3.93 kpc per arcsec.

2. X-ray & Optical Observations

2.1. Optical Observations

The optical observations were obtained with the Kitt Peak National Observatory’s 4m telescope equipped with the T2KB CCD camera at prime focus in 1995, February. This configuration delivered a plate scale of 0.47 arcsec per pixel. Images were exposed through the standard U plus liquid copper sulfate red-leak blocking filter, and an R -band filter with an effective wavelength of $\lambda 7431\text{\AA}$ that avoids contamination from strong emission lines. Exposure times were 2100 seconds in U and 1200 seconds in R . The target images were taken in short scan mode, which shifts charge in the CCD during an exposure to improve the flat field quality of the images. The target images were individually flat-fielded using twilight sky images; the bias level was subtracted from each image, and they were then combined into the science images used in our analysis. The seeing throughout the observations was $\simeq 2 - 3$ arcsec. The sky was transparent, and several photometric standard stars were observed throughout the evening.

2.2. Structure of the Central Galaxy

The R -band image of the central 40×40 arcsec (157×157 kpc) of the cluster is shown in Fig. 1a. The light is dominated by the central cluster cD galaxy located at RA = 14:01:02.01, Dec = +02:52:41.7 (J2000.0), and nearly two dozen fainter galaxies, several of which are projected onto the cD’s envelope. Fig. 1b shows the U -band image after subtracting a model of the background galaxy leaving only the blue starburst region at the center. The starburst is concentrated within a nine arcsec (35 kpc) radius of the nucleus. It is roughly circular in projection with no obvious resolved substructure or tidal features. The starburst is discussed further in Section 3.

The U - and R -band surface brightness profiles are presented in Fig. 2. The profiles were constructed using elliptical annuli with fixed ellipticities of 0.22 and position angles of $\simeq 331^\circ$, chosen by fitting the mean values of the R band isophotes beyond the starburst region. The surrounding galaxies were removed from the images in order to avoid contaminating the light of the cD. The surface brightness profiles in each band were flux calibrated using Landolt standards and transformed to the rest frame using K corrections from Coleman, Wu, & Weedman (1980). The K corrections in U and R are 1.176 mag and 0.258 mag respectively. Fluxes were corrected for Galactic foreground extinction using the prescriptions of Cardelli, Clayton, & Mathis (1989), assuming a foreground color excess of $E(B - V) = 0.03$. The profiles include statistical error bars (imperceptible in all but the outer points), and

systematic error confidence intervals (dashed lines) determined using the methods described in McNamara & O’Connell (1992).

The halo light beyond the starburst declines according to an $R^{1/4}$ profile. It rises above the extrapolation of the $R^{1/4}$ beyond 16 arcsec (63 kpc), where the characteristic cD halo becomes visible (Schombert 1986). Apart from the blue core, these properties are normal for central cluster galaxies within a redshift $z \lesssim 0.1$ (Porter et al. 1991).

In Fig. 3 we show the $(U - R)_{K,0}$ color profile derived from the surface brightness profiles. To establish a point of reference, the normal rest-frame colors for a cD galaxy generally lie within the range of 2.3 – 2.6 in the inner few tens of kpc, while the nuclear colors tend toward the red end of this range (Peletier et al. 1990). Fig. 3 shows that the cD’s $U - R$ color is anomalously blue in the inner 9 arcsec or so. It’s central color is approximately 1.3 magnitudes bluer than the halo color of $(U - R)_{K,0} \sim 2$ between 12 and 17 arcsec or so (47–67 kpc). The colors redden to a relatively normal color of $(U - R)_{K,0} \sim 2.3$ in the halo and envelope beyond 17 arcsec. This profile is the characteristic signature of a starburst, which we discuss in detail in Section 3.

2.3. Chandra X-ray Observations

The cluster was observed three times by Chandra: on December 11, 1999, for 19.5 ks (OBSID 495), on April 29, 2000, for 10.7 ks (OBSID 496), and again in December, 2005 for 66.5 ks. The 66.5 ks exposure, which we discuss in Section 4.3, is the first part of a longer, 250 ksec ACIS-I observation being made in pursuit of a separate project. The 1999 and 2000 images were made with the back-illuminated ACIS-S3 CCD. We analyzed this data using CIAO 3.2.3 with the calibrations of CALDB 3.1.0. The level 1 event files were reprocessed to apply the latest gain and charge transfer inefficiency correction and filtered for bad grades. The light curves of the resulting level 2 event files showed no strong flares in either observation. However, comparisons with XMM-Newton observations of Abell 1835 (Majerowicz et al. 2002, Jia et al. 2004) show that observation 495 was affected by a mild flare (see Markevitch 2002). This flare has the effect of significantly raising the modeled temperatures in the outer parts of the cluster (Schmidt, Allen, & Fabian 2001). We have therefore used only observation 496 for spectral analysis. However, since the flare is likely to be spatially uniform, we used both observations, appropriately corrected for exposure, for the imaging analysis.

The image of the combined 30 ks-equivalent exposure is shown in Figure 4. Outside of the core, the X-ray emission is fairly smooth and symmetrical in an elliptical distribution

with an ellipticity of ~ 0.12 and position angle of $\sim 340^\circ$. Inside the core, however, the emission is more complex, with twin, off-center peaks and two surface brightness depressions on either side of the cD’s nucleus (see Section 4.3).

To find the radial gas density and temperature distributions, we extracted spectra from observation 496 with at least 3000 counts in each concentric annulus about the X-ray centroid with the ellipticity and position angle given above. The appropriate blank-sky background file, normalized so that the count rate of the source and background images match in the 10–12 keV band, was used for background subtraction. In the following spectral analyses, all spectra were analyzed between the energies of 0.5 and 7.0 keV using XSPEC 11.3.2 (Arnaud 1996) and the spectra were binned with a minimum of 30 counts. To obtain temperatures and abundances, we used a model of a single-temperature plasma (MEKAL) plus the effects of Galactic absorption (WABS). Abell 1835 is located along the same line of sight as the Galactic North Polar Spur (Majerowicz et al. 2002), resulting in excess background at low energies. However, we are interested only in the bright inner parts of the cluster where the spur’s contribution to the background has a negligible effect on our fits. The redshift was fixed at $z = 0.253$, and the absorbing column density was fixed at the Galactic value of $N_H = 2.3 \times 10^{20} \text{ cm}^{-2}$ (Dickey & Lockman 1990). The temperature, abundance, and model normalization were allowed to vary. To investigate the effects of projection and to derive electron densities (n_e), we deprojected the spectra by including the PROJCT model in XSPEC with the single-temperature model (PROJCT×WABS×MEKAL) and by fitting all spectra simultaneously. We used the deprojected temperature and density ($n = 2n_e$) to determine the pressure ($P = nkT$), entropy ($S = kT/n^{2/3}$), and cooling time (Böhringer & Hensler 1989) of the gas in each annulus.

The profiles, shown in Figs. 5-8 are in overall agreement with the analyses of the same data by Markevitch (2002) and Schmidt, Allen, & Fabian (2001), and with the analyses of XMM-Newton data (e.g., Majerowicz et al. 2002, Jia et al. 2004). The temperature of the gas rises from ~ 4 keV in the center to ~ 11 keV at a distance of ~ 2 arcmin. As expected, the temperatures obtained from deprojection are slightly lower in the central regions than the projected temperatures, as the projected temperatures include emission from the hot outer parts of the cluster that is accounted for in deprojection. The abundance profile shows an increase towards the center, rising from approximately 1/3 of the solar abundance at a distance of ~ 2 arcmin to roughly solar abundance at the center. A spectrum extracted for the entire cluster within a radius of 3 arcmin gives an average, emission-weighted temperature of $kT = 7.8 \pm 0.3$ keV and abundance of $Z = 0.39 \pm 0.05 Z_\odot$.

The cooling rate of the gas was estimated by adding a cooling flow model (MKCFLOW) to the single-temperature model (i.e. WABS × [MEKAL+MKCFLOW]) and fitting it to

spectra extracted from the cooling region ($r_{\text{cool}} = 41$ arcsec), defined to be the region inside which the cooling time is $< 7.7 \times 10^9$ yr. Fits were made to both a single spectrum of the entire cooling region and to spectra extracted in concentric, deprojected elliptical annuli. In the latter case, to force all cooling to be within the cooling region, the MKCFLOW model normalization was set to zero outside the cooling region. For each spectrum, the temperature of the MEKAL component was tied to the high temperature of the MKCFLOW component, and the MEKAL and MKCFLOW abundances were tied together. Parameters were fixed or free to vary as described above.

We investigated several different cooling models. One explored the maximum cooling rate below the X-ray band allowed by the data. This model was constructed by fixing the low temperature of the cooling flow model to 0.1 keV. Another explored the maximum rate of cooling from roughly the mean gas temperature to the lowest detected temperature within the X-ray band by allowing the low temperature to vary. The first model found cooling limits as low as $\sim 30 M_{\odot} \text{ yr}^{-1}$, while the second model allowed for cooling at rates of several thousand solar masses per year. We also attempted to reproduce the cooling profile of Schmidt, Allen, & Fabian (2001) using newer calibration files, but were unable to do so. Because of the low exposure level and high particle background, it was difficult to find a stable and robust solution to the cooling models. We arrived at the conclusion that Peterson’s (2003) upper limit of $< 200 M_{\odot} \text{ yr}^{-1}$ is the most reliable measurement available, and we have adopted this value throughout the paper.

3. The Starburst in Abell 1835

3.1. Star Formation Rates from Near UV Imaging

Except where otherwise noted, our approach, methods, and rationale closely follow the discussion of the starburst in Abell 1068 (McNamara, Wise, & Murray 2004). Briefly, we estimate the luminosity, mass, and age of the starburst first by measuring the light emerging from the starburst population alone in the U and R bands. This involves modeling the light profile of the older background stellar population in each band and subtracting it from the respective image. The profiles generally follow an $R^{1/4}$ -law beyond the starburst, but the profiles soften considerably in the center of the galaxy where the true shape of the background light is poorly known. We therefore have taken two approaches that effectively give lower and upper bounds to the starburst population’s flux and color. The first involves an extrapolation of a spline fit to the halo profile into the core of the galaxy running underneath the starburst light (see McNamara, Wise, & Murray 2004 and references there). Second, we scaled the R band profile, which is minimally affected by the burst, to fit the U -band light profile

underneath the burst. Both models were subtracted from the images leaving the starburst in residual.

The ratios of the residual and model light give the fraction of light, $f(\lambda)$, contributed by the starburst population in each band. These methods give U -band light fractions of 25 per cent and 50 percent respectively within 9 arcsec of the nucleus. Since the real fraction depends on the true shape of the underlying light profile, we treat these values as lower and upper limits. In contrast, the starburst contributes only a few percent of the light at R . The starburst population mass is then found as $M_* = M/L(U)_* f(U)L(U)$, where $M/L(U)_*$ is the model-dependent U -band mass-to-light ratio of the starburst population, and $L(U)$ is its total U -band luminosity.

The starburst’s age is estimated by comparing its color to two simple but representative stellar population histories based on the Bruzual & Charlot (2003) population models: an instantaneous burst and continuous star formation, each of which assumes a Salpeter initial mass function and solar abundances (the choice of abundance has little effect on our results). We found the U -band luminosity of the starburst population alone to be $L(U)_* \equiv f(U)L(U) = 2.6 - 5.9 \times 10^{11} L_\odot$, before correcting for internal extinction. The intrinsic color of the starburst population provides a constraint on the population’s age, history, and mass-to-light ratio (see McNamara, Wise & Murray 2004). We find a probable range for the starburst population’s color of $(U - R)_* \sim -0.3$ to the bluest color that is theoretically possible $(U - R)_* \sim -1.4$.

The blue end of the color range is broadly consistent with an instantaneous burst that occurred less than 3 Myr ago involving a starburst population mass of between $9 \times 10^9 M_\odot$ and $2 \times 10^{10} M_\odot$. The red end of the color range is consistent with an aging, instantaneous burst that occurred 32 Myr ago, or ongoing (continuous) star formation for 320 Myr. The instantaneous and continuous starburst population masses are $2 \times 10^{10} M_\odot$ and $3 \times 10^{10} M_\odot$, respectively. The star formation rate for continuous star formation over the past 320 Myr is $100 M_\odot \text{ yr}^{-1}$. This is consistent with the spectroscopic rate found by Crawford et al. (1999), but somewhat lower than Allen’s (1995) rate.

The data are inconsistent with star formation that has been ongoing for $\gtrsim 1$ Gyr, as might be expected in a long-lived cooling flow (Fabian 1994), but the measurement uncertainties are too large to consider more complex star formation histories. The instantaneous burst model is always an unrealistic approximation. However, using colors alone we cannot rule-out an intense, short-lived burst of star formation fueled by a rapid infusion of gas supplied, perhaps, by a merger. Nevertheless, the enormous amount of molecular fuel ($\sim 10^{11} M_\odot$) that must be consumed by the starburst, even at the highest rates, suggests we are dealing with a longer-term event that is better described by continuous star formation

extending over several hundred Myr.

The U -band luminosities, masses, and star formation rates above have not been corrected for internal extinction. Doing so reliably requires high resolution images in two or more bands, which we do not have. Although no dust lanes are seen in our images, Crawford et al. (1999) estimated internal extinction at the level of $E(B - V) = 0.38$ based on anomalous Balmer emission-line ratios. Correcting this effect would increase the luminosity masses and the star formation rate above by a factor of about 1.8, giving a corrected star formation rate of $180 M_{\odot} \text{ yr}^{-1}$. The reddening would also affect the population colors, leading possibly to a somewhat younger age, which would lessen the accreted mass somewhat. A star formation rate between $100 - 180 M_{\odot} \text{ yr}^{-1}$ is broadly consistent with our data.

3.2. Far Ultraviolet, Infrared, and $H\alpha$ based Star Formation Rates

Other evidence for an ongoing starburst include the detections of $9 \times 10^{10} M_{\odot}$ of molecular gas (Edge 2001), and a far infrared 60μ flux of 330 ± 69 mJy (emission at 100μ is absent from the IRAS addscans). The corresponding far infrared luminosity of $L_{\text{FIR}}(60\mu\text{m}) = 3 \times 10^{45} \text{ erg s}^{-1}$, or $\sim 10^{12} L_{\odot}$, places Abell 1835 nearly in the class of ultra luminous infrared galaxies.

Assuming that the the far infrared and nebular emission are powered by star formation, they provide independent estimates of the star formation rate. Folding the infrared luminosity through Kennicutt’s (1998) relation, we find a star formation rate of $138 M_{\odot} \text{ yr}^{-1}$, a value that lies midway between the dust and dust-free U -band estimates.

Kennicutt’s relationship between $H\alpha$ luminosity and star formation rate gives a poorer match. Using the Crawford et al. (1999) $H\alpha$ luminosity $5.12 \times 10^{42} \text{ erg sec}^{-1}$, after correcting for internal extinction and different cosmologies, we arrive at a star formation rate of only $41 M_{\odot} \text{ yr}^{-1}$. This is substantially lower than the U -band and infrared continuum estimates. However the $H\alpha$ luminosity is an indirect and hence less reliable star formation indicator than the ultraviolet continuum.

Using the far UV imager on the XMM-Newton observatory, Hicks and Mushotzky (2005) found a star formation rate of $123 M_{\odot} \text{ yr}^{-1}$, which is consistent with our rate. As we do, they assumed a Salpeter IMF. However, lacking color information, they adopted a 900 Myr age for the population which is three times the age implied by the starburst population’s color. An age of 900 Myr implies a color of $(U - R) \sim 0$, which is three tenths of a magnitude redder than our measurement, but it lies at the limit of the uncertainty. If we adopt for the moment a 900 Myr old population with a corresponding U -band mass to light ratio of

~ 0.18 , we arrive at star formation rate of $50 M_{\odot} \text{ yr}^{-1}$. This rate is comparable to the $\text{H}\alpha$ rate, but it lies far below the infrared and nominal U -band rates. We regard this as a tight lower limit to the star formation rate in Abell 1835.

3.3. Abell 1835 and the Schmidt-Kennicutt Law for Star Formation

Using a large sample of disk galaxies and infrared-selected starburst galaxies, Kennicutt (1998) found a series of relationships between the surface densities of both molecular gas and star formation and the typical orbital periods of particles within the starburst regions. Normal disk galaxies, the centers of normal disks, and starburst galaxies spanning a broad range of gas and stellar surface densities lie along a series of relatively tight power-law relationships resembling the classical Schmidt (1959) law. This level of continuity suggests that the gross properties of star formation, such as the IMF, are not strongly effected by local environmental conditions.

It would therefore be worthwhile to compare cooling flow starbursts lying in high-pressure cluster cores with and without strongly interacting AGN to see if they follow global trends. We include in this comparison the cD in Abell 1068 which like Abell 1835 harbors a massive starburst (McNamara, Wise, & Murray 2004), but unlike Abell 1835 is apparently not currently experiencing an energetic AGN outburst. We measured the surface densities of star formation and molecular gas in both systems, and we calculated the orbital period at the edge of the star formation regions following Kennicutt’s (1998) prescription. Our results are listed in Table 1.

The values in Table 1 follow Kennicutt’s relationship between star formation rate density versus gas surface density $\Sigma_{\text{SFR}} \propto \Sigma_{\text{gas}}^{1.4}$ for starburst galaxies, normal disk galaxies, and the centers of normal disks. However, they are not located among the infrared starburst galaxies, as one might expect. Instead, they lie among the centers of normal disk galaxies. This is primarily due to the large spatial extent of the molecular gas (Edge & Frayer 2003) and star formation regions, which results in lower surface densities than the infrared starbursts in Kennicutt’s sample. This is true even though the cooling flow star formation rates dwarf those of spirals. At the same time, the orbital periods of stars at the edges of the cooling flow star formation regions are between 200 and 600 Myr, which is substantially longer than Kennicutt’s more compact starbursts. This implies that star formation is consuming the molecular gas before it has had time to execute more than a few orbits, which is again consistent with Kennicutt’s parameterizations and assumptions now routinely adopted in semi-analytical models of galaxy formation (eg., Kauffman 1996, Croton et al. 2006).

The molecular gas almost certainly originated outside of the cD. Whether it was stripped from a passing galaxy or whether it condensed out of the cooling flow is unknown. In the context of the cooling flow, its mass corresponds to approximately 4.5×10^8 years of accumulated gas from a $200 M_{\odot} \text{ yr}^{-1}$ flow. This timescale is close to both the cooling and orbital timescales within the starburst. The gas may have pooled following an interruption in a time dependent cooling flow, as might be expected in AGN-regulated systems. Alternatively, it may be that the molecular gas accumulated at the center of the galaxy until it reached a critical density for the onset and maintenance of star formation. If so, the apparent agreement between the cooling and star formation rates implies that the cooling gas is feeding the reservoir of molecular gas now at about the mean rate it has done so for the past several hundred Myr.

It is worth noting that earlier suggestions that the high ambient pressure in cooling flows might alter the Jean’s unstable molecular cloud mass leading to an anomalous IMF (e.g. Sarazin & O’Connell 1983) are not supported by this analysis. Furthermore, with growing evidence for feedback-driven quenching of cooling flows, it is no longer necessary to appeal to a faint stellar repository that would justify the need for an anomalous IMF.

3.4. Chemical Enrichment from the Starburst

Metal enrichment by a starburst of this size is significant enough to enhance the metallicity of the gas in the core. Fig. 8 shows the metal abundance rising from roughly 1/3 of the solar abundance at 200 kpc to nearly solar metallicity in the starburst region. A similar rise but with a somewhat smaller amplitude (and poorer spatial resolution) was also seen in an XMM-Newton analysis of Abell 1835 by Majerowicz, Neuman, & Reiprich (2002). Their XMM observation follows the metallicity profile out to about 800 kpc, where the cluster’s average metallicity is about 1/4 of the solar value. The metallicity begins to rise at a radius of about 160 kpc (50 arcsec), which is beyond the edge of our profile in Fig. 8. Following the procedure of Wise, McNamara, & Murray (2004), we find that the starburst alone is capable of enriching the gas in the inner 160 kpc from 1/4 of the solar value to the solar value without difficulty. In fact, the starburst is considerably more compact than the metal-enhanced central region of the cluster. Were the metals produced by the starburst confined to the star formation region, the hot gas would become enriched to levels well above the solar value, which is not observed. This problem might be circumvented if the metal-rich gas produced by the burst has been transported outward and mixed with the lower metallicity gas in the halo by a merger or an outflow driven by the AGN. Alternatively, the metals produced in the starburst may be primarily locked in the cold gas and are unable to enhance

the metallicity of the hot gas. Finally, the observed metallicity gradient could have been imprinted by stellar evolution of the cD’s older population (De Grandi et al. 2004). This issue will be explored further in a future paper.

3.5. Comparison Between the Cooling Rate and Star Formation Rate

The starburst in Abell 1835 sits in a region where the cooling time has fallen below 6×10^8 yr, which is close to the age of the starburst. The temperature of the gas has also reached a minimum of 3.5 keV there, which is similar to other cooling flow systems, such as Hydra A (McNamara et al. 2000) and Abell 1068 (McNamara, Wise, & Murray 2004). These conditions are qualitatively consistent with expectations for fueling by the cooling flow. However, quantitative consistency requires that there be mass continuity between the rate of cooling and its sink. The vast gulf between radiative cooling rates and star formation cast a pall on the pure (no feedback) cooling flow model since it was conceived nearly 30 years ago.

An observation made with XMM-Newton’s reflection grating spectrometer (Peterson et al. 2003) shows that the gas in Abell 1835 is cooling at a rate of between $1000\text{--}2000 M_{\odot} \text{ yr}^{-1}$ from the mean gas temperature of nearly 9 keV to about 2 keV where cooling slows dramatically (Peterson et al. 2003). Below 2 keV, cooling proceeds at a much reduced rate of $\lesssim 200 M_{\odot} \text{ yr}^{-1}$. Whether any cooling out of the X-ray band occurs is still to be demonstrated. However, cooling at this reduced rate is now consistent with the star formation rate in the cD galaxy. Provided there is an active heating mechanism to offset the remaining cooling luminosity, which we justify below, the (reduced) cooling model is now consistent with a sink in star formation and the central black hole. This situation is evidently true in an increasing fraction of cooling flow clusters (Rafferty et al. 2006).

4. Feedback & Regulated Cooling in the Cluster’s Core

The data discussed in the previous section are consistent with an active but relatively moderate cooling flow. Nevertheless, the gas throughout the central 150 kpc of the cluster has a cooling time that is shorter than the cluster’s age (Fig. 7), yet most of this gas is not condensing out. The radiation losses from this gas,

$$L_{\text{cool}} \simeq 1.2 \times 10^{45} \left(\frac{\dot{M}}{1000 M_{\odot} \text{ yr}^{-1}} \right) \text{ erg sec}^{-1}, \quad (1)$$

must then be replenished by heating (Fabian et al. 2001, Böhringer et al. 2001). We now consider whether thermal conduction, the AGN, and supernova explosions are able to compensate the radiative losses.

4.1. Feedback from the Starburst

Here we adopt an optimistic star formation rate of $180 M_{\odot} \text{ yr}^{-1}$, and we follow closely the discussions in McNamara, Wise, & Murray (2004), and Wise, McNamara, & Murray (2004). We assume a blast energy per type 2 supernova of 10^{51} erg, and a type 2 supernova production rate of one per $127 M_{\odot}$ of star formation (Hernquist & Springel 2003). These values then yield an average energy injection rate over the life of the starburst of $4.5 \times 10^{43} \text{ erg s}^{-1}$. This is at most a few percent of the power required to quench the cooling flow, even with efficient coupling between the supernova blast energy and the hot gas. This figure can be boosted by adopting an extreme supernova yield per mass, or an IMF richer in massive stars than the Salpeter function. However, the requirements are still extreme in view of earlier arguments weighing against an IMF that is dramatically different from Salpeter's. Supernovae may be an important source of heat in the region surrounding the starburst and AGN, but they cannot have a substantial effect on the overall cooling flow. The same conclusion was reached for the Abell 1068 cluster cD (McNamara, Wise, & Murray 2004). Since both are among the most massive starbursts known in cooling flows, this conclusion probably holds in most systems.

4.2. Heating by Thermal Conduction

The conditions in which inward-flowing heat from the hot layers of gas surrounding the cooling core are able to replenish radiation losses have been studied extensively in recent years (Fabian, Voigt, & Morris 2002, Zakamska & Narayan 2003, Voigt & Fabian 2004). Abell 1835 has been examined in this context but with contradictory results. Zakamska & Narayan (2003) were apparently able to construct theoretical gas temperature, density, and cooling profiles that matched those of Abell 1835 using an inward heat flux proceeding at 40 per cent of the Spitzer rate. On the other hand Voigt & Fabian (2004) found that heat conduction proceeding at a modest fraction of the Spitzer rate could quench cooling only in the outer reaches of the cooling region, but not near the central starburst where the gas temperature is rapidly decreasing. In order to balance radiative losses, they found that the conductivity must exceed the Spitzer value within the radius at which the gas falls below 7 keV. The conductivity reaches 1/3 of the Spitzer value where the gas temperature is approximately 10

keV. The corresponding radii are 20 arcsec (79 kpc) and 40 arcsec (157 kpc), respectively. It seems reasonable then to expect thermal conduction to balance radiation losses in the outer parts of the cooling region, but to be unable to do so in the central region near the starburst. Although similar conclusions were reached for the Abell 1068 cluster (Wise, McNamara, & Murray 2004), the importance of conduction without knowledge of the conductivity of the gas is difficult to evaluate with confidence.

4.3. AGN Feedback: X-ray Cavities

The structure in the inner 10 arcsec of the X-ray image shown in Fig. 9 was first reported by Schmidt, Allen, & Fabian (2001), who attributed it, we now believe incorrectly, to a recent merger. Two surface brightness depressions with count deficits of approximately 20% to 40% compared to the surrounding emission are seen in the ACIS-S images 6 arcsec (23 kpc) to the north-west and 5 arcsec (17 kpc) to the south-east of the cD’s nucleus. The cavities were confirmed by the 66.5 ksec ACIS-I image shown at left in Fig. 9. The nucleus lies in the trough between the two bright central knots of emission. The trough might be caused by photoelectric absorption of X-rays by the molecular gas clouds. The cavities have bright rims and otherwise resemble the AGN-induced X-ray cavities now seen in more than two dozen clusters (Rafferty et al. 2006, Bîrzan et al. 2004, Dunn & Fabian 2005). Their physical characteristics are given in Table 2, including their distances from the nucleus, the sizes of their major and minor axes, the surrounding gas pressures and deprojected temperatures, the $1pV$ energies of the cavities, and the approximate buoyancy ages (see Bîrzan et al. 2004).

We were initially concerned that the cavities themselves might be caused by photoelectric absorption from the molecular gas in the cD. Edge & Frayer (2003) found a column density of $4 \times 10^{22} \text{ cm}^{-2}$ in the inner 10 kpc region of the cD, which is centrally concentrated and does not correspond to the two off-axis surface brightness depressions. We found a small excess column density of $\sim 3 \times 10^{21} \text{ cm}^{-2}$ from the X-ray spectrum of the inner 10 arcsec or so, as do Schmidt, Allen, & Fabian (2001), which could be the diluted column of molecular gas. However, because the cavities are seen in both hard and soft images above and below 2 keV, they cannot be due to photoelectric absorption, which dominates below 2 keV.

The sizes of the cavities are more or less typical of those found in massive clusters (e.g., Bîrzan et al. 2004, Dunn & Fabian 2004). However, the central pressure of $1.1 \times 10^{-9} \text{ erg cm}^{-3}$ is more than an order of magnitude larger than is typically found at the base of a cooling flow. The work required to inflate the cavities against the surrounding pressure is $pV = 4.3 (-1.5, +4.6) \times 10^{59} \text{ erg}$. This corresponds to a mean mechanical power of $L = 3.5 (-1, +3.0) \times 10^{44} \text{ erg s}^{-1}$, assuming a rise time of about 40 Myr. The total

enthalpy is roughly 2.5 to 4 times larger, depending on the equation of state of the gas filling the cavity (Bîrzan et al. 2004). This implies a total jet power of $\sim 1.4 \times 10^{45}$ erg s $^{-1}$, which is comparable to the cooling luminosity of a 1000 – 2000 M_{\odot} yr $^{-1}$ cooling flow. So long as the coupling between the AGN and the gas is reasonably efficient, the AGN power is high enough to offset radiation losses in this system.

The cD harbors a compact radio source shown in Fig. 9. The image obtained from the Very Large Array archive was taken in the A configuration at a frequency of 1.4 GHz. The resolution of the image is about one arcsec. The spectral index $\alpha = 0.65$ ($f_{\nu} \propto \nu^{-\alpha}$) implies a total radio luminosity of $3.55 \pm 0.09 \times 10^{41}$ erg s $^{-1}$ between 10 MHz and 10 GHz. (A more complete discussion of the radio properties will be given in a forthcoming paper.) The radio source at this frequency shows no obvious connection to the cavity system; however, the 330 MHz map (also discussed in a forthcoming paper) covers the entire extent of the cavities, but again shows no detailed correlation with the holes. The low frequency source is probably the remnant synchrotron emission from the outburst which occurred about 40 Myr ago.

The nucleus of Abell 1835 is a striking example of how poorly radio synchrotron emission traces true jet power. The average jet power required to inflate the cavities, $\sim 1.4 \times 10^{45}$ erg s $^{-1}$, dwarfs the total radio synchrotron power, exceeding it by a factor of 4000. The corresponding synchrotron radiative efficiency is then only about 0.02%, which is vastly smaller than $\sim 1\%$ found for M87 (Owen et al. 2000) and other sources (De Young 1993, Bicknell, Dopita, & O’Dea 1997).

5. Simultaneous Growth of the Bulge and the Supermassive Black Hole

The magnitude of the AGN outburst implies that the central black hole has accreted $\simeq 4pV/\epsilon c^2 = 1.1 \times 10^7 M_{\odot}$ ($\epsilon = 0.1$) in the past 40 Myr or so, corresponding to an average accretion rate of $\sim 0.3 M_{\odot}$ yr $^{-1}$ (Rafferty et al. 2006). Adopting the star formation rate as an estimate of the current bulge growth rate (see Rafferty et al. 2006 for a more detailed discussion), we find that the bulge has added between 300 and 600 units of mass for every one unit that has fallen into the black hole. This relative growth rate is intriguingly close to the slope of the Magorrian relation between bulge and black hole mass in quiescent galaxies (Håring & Rix 2004). The convergence of several factors, including the fact that star formation in the cD is proceeding at a rate that rivals or exceeds those observed during the peak years of galaxy formation (Juneau et al. 2005), suggests that the physical conditions driving this growth could be analogous to those that held in the early universe when the Magorrian relation was presumably imprinted on galaxies. The cooling flow systems probably differ, however, in that their accretion is substantially sub-Eddington. The conditions in

Abell 1835 should be placed in context with similar systems, which clearly show a trend between star formation and black hole growth, but there is a great deal of scatter (Rafferty et al. 2006). In some systems the black hole has grown by a substantial fraction of its mass in a single outburst but with little commensurate bulge growth over the same time period (McNamara et al. 2005, Nulsen et al. 2005 a). In other systems, such as Abell 1068 (McNamara, Wise, & Murray 2004), the bulge is growing much faster than the black hole. In general, cooling flow cDs and their black holes have evidently not grown in lock-step over the past several Gyr (Rafferty et al. 2006).

6. Summary & Discussion

The cD galaxy in Abell 1835 is in the midst of a starburst proceeding at a rate of $100 - 180 M_{\odot} \text{ yr}^{-1}$ that began approximately 320 Myr ago. The star formation rate is consistent with the maximum rate that gas can be condensing out of the cooling flow. Cooling and accretion at this level can account for only 10% to 20% of the total radiative losses, implying that the bulk the gas is being heated and maintained at X-ray temperatures. Supernovae in the starburst are energetically incapable of producing enough heat to do so, and thermal conduction is ineffective in the inner regions of the cooling flow.

We discovered a pair of cavities in the hot gas produced by a powerful AGN outburst that occurred roughly 40 Myr ago. The outburst was energetic enough to offset the remaining radiative losses. There is no longer a discrepancy between the radiative cooling rate and the sink of the cooling gas, provided the jet power heats the gas efficiently. The jet power required to produce the cavities exceeds the radio synchrotron power by $\simeq 4000$ times, indicating a radiatively inefficient yet powerful radio source.

The jet power $1.4 \times 10^{45} \text{ ergs s}^{-1}$ corresponds to the Eddington luminosity of a $\sim 10^7 M_{\odot}$ black hole. However, the K-band luminosity of the host cD galaxy implies a much larger black hole mass of approximately $5 \times 10^9 M_{\odot}$ (Rafferty et al. 2006), implying that accretion is proceeding at a small fraction $\sim 3 \times 10^{-3}$ of the Eddington rate. This exceeds the Bondi rate by nearly 500 times, assuming the measured central gas density holds near the unresolved Bondi radius (Rafferty et al. 2006). Minding the uncertain assumptions about the black hole mass and surrounding gas density, Bondi accretion could contribute at some level, but is unlikely to be primarily responsible for feeding the outburst. The large pool of centrally condensed molecular gas is consistent with cold accretion. If the molecular gas is fed by gas condensing out of the hot phase, it would provide a natural supply of fuel necessary to maintain an AGN feedback loop. We cannot, however, exclude the possibility that the gas arrived through a merger.

The rate of black hole growth implied by the jet power and bulge growth through star formation are consistent with the slope of the (Magorrian) relationship between bulge mass and black hole mass for quiescent bulges. This surprising result suggests that feedback processes like those operating in this system could be driving the relationship between bulge mass and supermassive black hole mass in normal bulges (Magorrian et al. 1998, Kormendy & Richstone 1995, Springel DiMatteo & Hernquist 2005). In a large sample of cooling flows, Rafferty et al. (2006) have found a trend between bulge growth rate through star formation and black hole growth rate over the past \sim Gyr. However, the large scatter in the relative rates implies that bulge and black hole growth do not always proceed in lock-step. This result also supports the growing consensus that AGN feedback could explain the exponential decline in luminous galaxies relative to the predicted shape of the dark matter halo mass function by suppressing cooling (Benson et al. 2003, Croton et al. 2006, Best et al. 2006). Consequently, the mode of accretion in this and other cooling flow systems should hold considerable interest to more general models of galaxy formation (e.g., Croton et al. 2006, Soker 2006, Pizzolato & Soker 2005, Sijacki & Springel 2006).

Abell 1835’s nuclear outburst is as powerful as a quasar’s and its starburst is proceeding at a rate that rivals those in burgeoning galaxies beyond $z = 2$. However, there are noteworthy differences in the way the gravitational binding energy of accretion is channeled away from the black hole. While quasars radiate away most of their accretion energy, the accretion energy emerging from Abell 1835 and other cooling flows is almost entirely mechanical. Abell 1835’s jet power $\sim 1.4 \times 10^{45}$ ergs s^{-1} exceeds postulated protogalactic wind luminosities (Silk & Rees 1998) by an order of magnitude, as it must to all but stop the cooling flow. However, strong nonthermal nuclear emission and broad emission lines are absent, and the radiative efficiency of the radio source, defined as the ratio of radio synchrotron power to jet power, is very low. This may be a characteristic of the late stages of galaxy formation when accretion onto the black hole falls below the Eddington rate which probably held during the early stages of galaxy formation (Silk & Rees 1998, Blandford 1999, Begelman & Nath 2005, Churazov et al. 2005). Even so, long-lived accretion at the present rate would continue to drive star formation and black hole growth such that the relationship between bulge and black hole mass found in quiescent ellipticals would be imprinted or maintained.

Following a checkered and often contentious history, the cooling flow problem is now coming to resolution. We should emphasize, however, that the model must still pass an essential test. Gas cooling out of the intracluster medium should emit detectable X-ray cooling lines, notably the Fe XVII line at 15\AA (0.826 keV). In this case, the flux scales as

$$f(FeXVII) = 5.456 \times 10^{-15} \left(\frac{\dot{M}}{100 M_{\odot} \text{ yr}^{-1}} \right) \left(\frac{D}{500 \text{ Mpc}} \right)^{-2} \text{ ergs s}^{-1} \text{ cm}^{-2} \quad (2)$$

where D is the distance and \dot{M} is the cooling rate. Peterson's et al (2003) limits successfully ruled-out wholesale cooling but they generally lie well above the levels of accretion implied by the observed star formation rates (Rafferty et al. 2006). A cooling rate \dot{M} approximately equal to the observed star formation rates is currently detectable using deep XMM-Newton observations and will be in the future using shorter observations with the Constellation-X observatory. For the half dozen or so objects whose star formation rates are comparable to the available cooling upper limits (including Abell 1835 and Abell 1068), a 200 – 400 ksec XMM observation using the reflection grating spectrometer would be sufficient to restrictively test the cooling flow/feedback model of galaxy formation.

This research was funded by NASA Long Term Space Astrophysics Grant NAG4-11025.

REFERENCES

- Allen, S. W. 1995, MNRAS, 276, 947
- Allen, S. W., Fabian, A. C., Edge, A. C., Bautz, M. W., Furuzawa, A., & Tawara, Y. 1996, MNRAS, 283, 263
- Arnaud, K. A. 1996, in ASP Conf. Ser. 101, Astronomical Data Analysis Software and Systems V, ed. G. H. Jacoby & J. Barnes (San Francisco: ASP), 17
- Balogh, M. L., Pearce, F. R., Bower, R. G., & Kay, S. T. 2001, MNRAS, 326, 1228
- Basson, J. F., & Alexander, P. 2003, MNRAS, 339, 353
- Begelman, M. C., & Nath, B. B. 2005, MNRAS, 361, 1387
- Benson, A. J., Bower, R. G., Frenk, C. S., Lacey, C. G., Baugh, C. M., & Cole, S. 2003, ApJ, 599, 38
- Bertschinger, E., & Meiksin, A. 1986, ApJ, 306, L1
- Best, P. N. et al. 2006, astro-ph/0602171
- Bicknell, G. V., Dopita, M. A., & O'Dea, C. P. O. 1997, ApJ, 485, 112
- Binney, J. 2004, Phil Trans Roy Soc A363 (2005) 739-749 (astro-ph/0407238)
- Bîrzan, L., Rafferty, D. A., McNamara, B. R., Wise, M. W., & Nulsen, P. E. J. 2004, ApJ, 607, 800

- Blanchard, A., Valls-Gabaud, D., & Mamon, G. A. 1992, *A&A*, 264, 365
- Blanton, E. L., Sarazin, C. L., & McNamara, B. R. 2003, *ApJ*, 585, 227
- Blandford, R. D. 1999, in *Galaxy Dynamics*, ed. Merritt, Valuri, and Sellwood, ASP conf. ser. (astro-ph/9906025)
- Böhringer, H., Hensler, G. 1989, *A&A*, 215, 147
- Böhringer, H., Matsushita, K., Churazov, E., Ikebe, Y., & Chen, Y. 2002, *A&A*, 382, 804
- Borgani, S., Governato, F., Wadsley, J., Menci, N., Tozzi, P., Quinn, T., Stadel, J., & Lake, G. 2002, *MNRAS*, 336, 409
- Brighenti, F., & Mathews, W. G. 2002, *ApJ*, 573, 542
- Brüggen, M. 2003, *ApJ*, 592, 839
- Brüggen, M., & Kaiser, C. R. 2001, *MNRAS*, 325, 676
- Brüggen, M., & Kaiser, C. R. 2002, *Nature*, 418, 301
- Bruzual, G., & Charlot, S. 2003, *MNRAS*, 344, 1000
- Cardelli, J. A., Clayton, G. C., & Mathis, J. S. 1989, *ApJ*, 345, 245
- Churazov, E., Brüggen, M., Kaiser, C. R., Böhringer, H., & Forman, W. 2001, *ApJ*, 554, 261
- Churazov, E., Sunyaev, R., Forman, W., Böhringer, H. 2002, *MNRAS*, 332, 729
- Churazov, E., Sazonov, S., Sunyaev, R., Forman, W., Jones, C., & Böhringer, H. 2005, *MNRAS*, 363, L91
- Ciotti, L., & Ostriker, J. P. 1997, *ApJ*, 487, L105
- Cole, S. 1991, *ApJ*, 367, 45
- Coleman, G. D., Wu, C.-C., & Weedman, D. W. 1980, *ApJS*, 43, 393
- Cowie, L. L. & Binney, J. 1977, *ApJ*, 215, 723
- Crawford, C. S., Allen, S. W., Ebeling, H., Edge, A. C., & Fabian, A. C. 1999, *MNRAS*, 306, 857
- Crawford, C. S., Sanders, J. S., Fabian, A. C. 2005, *MNRAS*, 361, 17

- Croton, D. J., Springel, V., White, S. D. M., et al. 2005, astro-ph/0508046
- Baker, K. 2005, MNRAS, 360, 748
- David, L. P., Nulsen, P. E. J., McNamara, B. R., Forman, W., Jones, C., Ponman, T., Robertson, B., & Wise, M. 2001, ApJ, 557, 546
- De Grandi, S., Etti, S., Longhetti, M., & Molendi, S. 2004, A&A, 419, 7
- De Young, D. S. 1993, ApJ, 402, 95
- De Young, D. S. 2003, MNRAS, 343, 719
- Dickey, J. M., & Lockman, F. J. 1990, ARA&A, 28, 215
- Donahue, M., Mack, J., Voit, G. M., Sparks, W., Elston, R., & Maloney, P. R. 2000, ApJ, 545, 670
- Donahue, M. et al. 2005, astro-ph/0511401
- Dunn, R. J. H. & Fabian, A. C. 2004, MNRAS, 355, 862
- Edge, A. C. 2001, MNRAS, 328, 762
- Edge, A. C. & Frayer, D. T. 2003, ApJ, 594, L13
- Fabian, A. C. 1994, ARA&A, 32, 277
- Fabian, A. C., Mushotzky, R. F., Nulsen, P. E. J., & Peterson, J. R. 2001, MNRAS, 321, L20
- Fabian, A. C., Sanders, J. S., Crawford, C. S., Conselice, C. J., Gallagher, J. S., Wyse, R. F. G. 2003, MNRAS, 344, 48
- Fabian, A. C. & Nulsen, P. E. J. 1977, MNRAS 180, 479
- Fabian, A. C. 1999, MNRAS, 308, L 39
- Fabian, A. C., Voigt, L. M., & Morris, R. G. 2002, MNRAS, 335, L71
- Fabian, A. C., Sanders, J. S., Allen, S. W., Crawford, C. S., Iwasawa, K., Johnstone, R. M., Schmidt, R. W., & Taylor, G. B. 2003, MNRAS, 344, L43
- Falcke, H., Rieke, M. J., Rieke, G. H., Simpson, C., & Wilson, A. S. 1998, ApJ, 494, L155
- Ferrarese, L., & Merritt, D. 2000, ApJ, 539, L9

- Finoguenov, A., & Jones, C. 2001, *ApJ*, 547, L107
- Forman, W., et al. 2005, *ApJ*, 635, 894
- Gallagher, J. S. & Ostriker, J. P. 1972, *AJ*, 77, 288
- Gebhardt, K., et al. 2000, *ApJ*, 539, L13
- Gómez, P. L., Loken, C., Roettiger, K., & Burns, J. O. 2002, *ApJ*, 569, 122
- Häring, N. & Rix, H. W. 2004, *ApJ*, 604, L89
- Hausman, M. A. & Ostriker, J. P. 1978, 224, 320
- Heckman, T. M., Baum, S. A., van Breugel, W. J. M., & McCarthy, P. 1989, *ApJ*, 338, 48
- Heinz, S., Choi, Y.-Y., Reynolds, C. S., & Begelman, M. C. 2002, *ApJ*, 569, L79
- Hernquist, L., & Springel, V. 2003, *MNRAS*, 341, 1253
- Hicks, A. K., & Mushotzky, R. 2005, *ApJ*, 635, L9
- Jaffe, W. 1990, *A & A*, 240, 254
- Jaffe, W., Bremer, M. N., & Baker, K. 2005, *MNRAS*, 360, 748
- Jaffe, W., Bremer, M. N., & van der Werf, P. P. 2001, *MNRAS*, 324, 443
- Jia, S. M., Chen, Y., Lu, F. J., & Xiang, F. 2004, *A&A*, 423, 65
- Johnstone, R. M., Fabian, A. C., & Nulsen, P. E. J. 1987, *MNRAS*, 224, 75
- Jones, T. W., & De Young, D. S. 2005, *ApJ*, 624, 586
- Juneau, J., Glazebrook, K., Crampton, D., McCarthy, P. J. et al. 2005, *ApJ*, 619, L135
- Kaiser, C. R., & Binney, J. 2003, *MNRAS*, 338, 837
- Kauffmann, G. 1996, *MNRAS*, 281, 475
- Kennicutt, R. C. 1998, *ApJ*, 498, 541
- Kormendy, J. & Richstone, D. 1995, *ARAA*, 33, 581
- Kraft, R. P. et al. 2005, *astro-ph/0511797*
- Magorrian, J., et al. 1998, *AJ*, 115, 2285

- Markevitch, M. 2002, preprint (astro-ph/0205333)
- Markevitch, M., & Vikhlinin, A. 2001, *ApJ*, 563, 95
- Majerowicz, S., Neumann, D. M., & Reiprich, T. H. 2002, *A&A*, 394, 77
- McNamara, B. R., et al. 2000, *ApJ*, 534, L135
- McNamara, B. R., O’Connell, R. W., & Bregman, J. N. 1990, *ApJ*, 360, 20
- McNamara, B. R., Nulsen, P. E. J., Wise, M. W., Rafferty, D. A., Carilli, C., Sarazin, C. L., & Blanton, E. L. 2005, *Nature*, 433, 45
- McNamara, B. R., & O’Connell, R. W. 1989, *AJ*, 98, 2018
- McNamara, B. R., & O’Connell, R. W. 1992, *ApJ*, 393, 579
- McNamara, B. R., & O’Connell, R. W. 1993, *AJ*, 105, 417
- McNamara, B. R., et al. 2001, *ApJ*, 562, L149
- McNamara, B. R., Wise, M. W., & Murray, S. S. 2004, *ApJ*, 601, 173
- McNamara, B. R. 2004, in, "The Riddle of Cooling Flows in Galaxies and Clusters of Galaxies", eds. Reiprich, T. H., Kempner, J. C., & Soker, N., Charlottesville, VA, USA (astro-ph/0402081)
- Merritt, D. 1985, *ApJ*, 289, 18
- Metzler, C. A. & Evrard, A. E. 1994, *ApJ*, 437, 564
- Molendi, S., & Pizzolato, F. 2001, *ApJ*, 560, 194
- Narayan, R., & Medvedev, M. V. 2001, *ApJ*, 562, L129
- Nulsen, P. E. J., David, L. P., McNamara, B. R., Jones, C., Forman, W. R., & Wise, M. 2002, *ApJ*, 568, 163
- Nulsen, P. E. J., Hambrick, D. C., McNamara, B. R., Rafferty, D., Birzan, L., Wise, M. W., & David, L. P. 2005, *ApJ*, 625, L9 (a)
- Nulsen, P. E. J., McNamara, B. R., Wise, M. W., & David, L. P. 2005, *ApJ*, 628, 629 (b)
- O’Dea, C. P., Baum, S. A., & Gallimore, J. F. 1994, *ApJ*, 436, 669
- Omnia, H., Binney, J., Bryan, G., & Slyz, A. 2004, *MNRAS*, 348, 1105

- Owen, F. N., Eilek, J. A., & Kassim, N. E. 2000, *ApJ*, 543, 611
- Peletier, R. F., Davies, R. L., Illingworth, G. D., Davis, L. E., & Cawson, M. 1990, *AJ*, 100, 1091
- Peterson, J. R., et al. 2001, *A&A*, 365, L104
- Peterson, J. R., Kahn, S. M., Paerels, F. B., Kaastra, J. S., Tamura, T., Bleeker, J. A. M., Ferrigno, C., & Jernigan, J. G. 2003, *ApJ*, 590, 207
- Piffaretti, R. & Kaastra, J. S. 2006, astro-ph/0602376
- Pizzolato, F., & Soker, N. 2005, *ApJ*, 632, 821
- Porter, A. C., Schneider, D. P., & Hoessel, J. G. 1991, *AJ*, 101, 1561
- Quilis, V., Bower, R. G., & Balogh, M. L. 2001, *MNRAS*, 328, 1091
- Rafferty, D. A. et al. 2006, *ApJ*, submitted
- Reynolds, C. S., Heinz, S., & Begelman, M. C. 2002, *MNRAS*, 332, 271
- Ruszkowski, M., & Begelman, M. C. 2002, *ApJ*, 581, 223
- Ruszkowski, M., Brüggem, & Begelman, M. 2004, *ApJ*, 615, 675
- Rosner, R., & Tucker, W. H. 1989, *ApJ*, 338, 761
- Salomé, P., & Combes, F. 2003, *A&A*, 412, 657
- Sarazin, C. L., & O'Connell, R. W. O. 1983, *ApJ*, 268, 560
- Sarazin, C. L. 1986, *Rev. Mod. Phys.*, 58, 1
- Schmidt, M. 1959, *ApJ*, 129, 243
- Schmidt, R. W., Allen, S. W., & Fabian, A. C. 2001, *MNRAS*, 327, 1057
- Schombert, J. M. 1986, *ApJS*, 60, 603
- Sijacki, D., Springel, V. 2006, *MNRAS*, 366, 397
- Silk, J., Djorgovski, S., Wyse, R. F. G., & Bruzual A., G. 1986, *ApJ*, 307, 415
- Silk, J. & Rees, M. 1998, *A&A*, 331, L1
- Soker, N. 2006 (astro-ph/0602043)

- Soker, N., Blanton, E. L., & Sarazin, C. L. 2002, *ApJ*, 573, 533
- Soker, N., White, R. E., David, L. P., & McNamara, B. R. 2001, *ApJ*, 549, 832
- Springel, V., Di Matteo, T., & Hernquist, L. 2005, *MNRAS*, 361, 776
- Tabor, G., & Binney, J. 1993, *MNRAS*, 263, 323
- Tamura, T., et al. 2001, *A&A*, 365, L87
- Taylor, G. B. 1996, *ApJ*, 470, 394
- Tucker, W. H., & Rosner, R. 1983, *ApJ*, 267, 547
- Vernaleo, J. C. & Reynolds, C. S. 2005, *astro-ph/0511501*
- Voigt, L. M., & Fabian, A. C. 2004, *MNRAS*, 347, 1130
- Voigt, L. M., Schmidt, R. W., Fabian, A. C., Allen, S. W., & Johnstone, R. M. 2002, *MNRAS*, 335, L7
- Voit, G. M., & Donahue, M. 1997, *ApJ*, 486, 242
- Voit, G. M. 2004, *Rev. Mod. Phys.*, in press (*astro-ph/0410173*)
- Voit, G. M., & Donahue, M. 2005, *ApJ*, 634, 955
- White, S. D. M., & Rees, M. J. 1978, *MNRAS*, 183, 341
- Wise, M. W., McNamara, B. R., & Murray, S. S. 2004, *ApJ*, 601, 184
- Wu, K. K. S., Fabian, A. C., & Nulsen, P. E. J. 2000, *MNRAS*, 318, 889
- Young, A. J., Wilson, A. S., & Mundell, C. G. 2002, *ApJ*, 579, 560
- Zakamska, N. L., & Narayan, R. 2003, *ApJ*, 582, 162

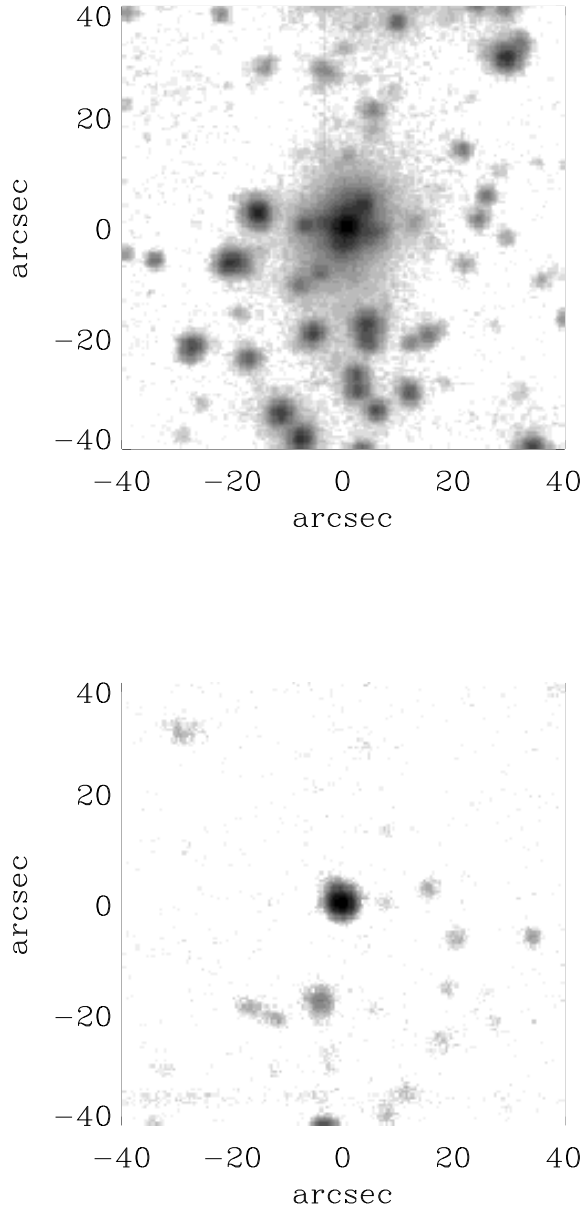


Fig. 1.— Fig. 1- **a** R-band image of the 40×40 arcsec (157×157 kpc) region of the cluster centered on the cD galaxy. **b** U-band image of the same region, but with the background population of the cD removed showing the central starburst.

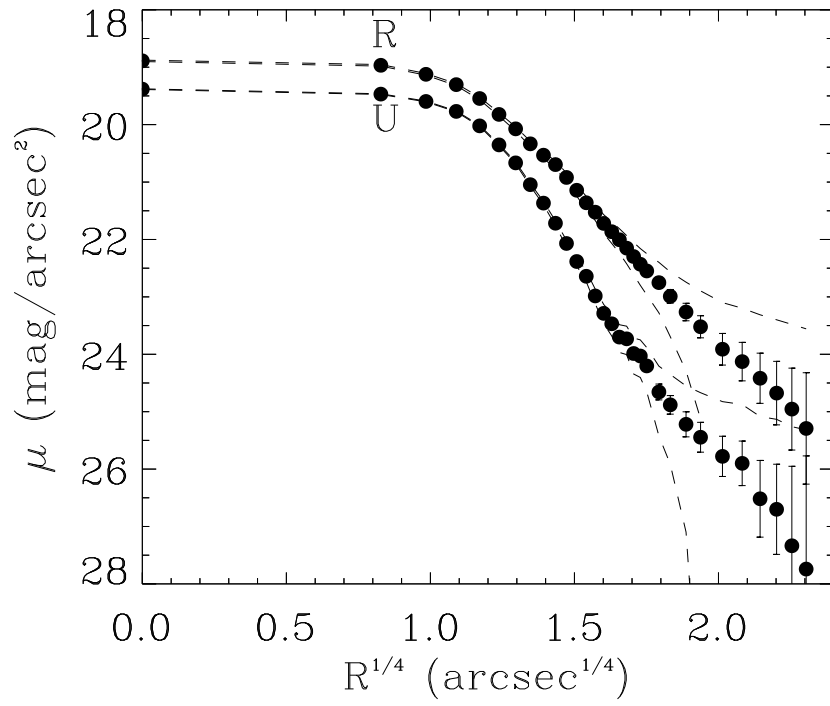


Fig. 2.— U-band and R-band surface brightness profiles of the cD galaxy. The dashed lines represent the systematic uncertainty associated with sky background subtraction

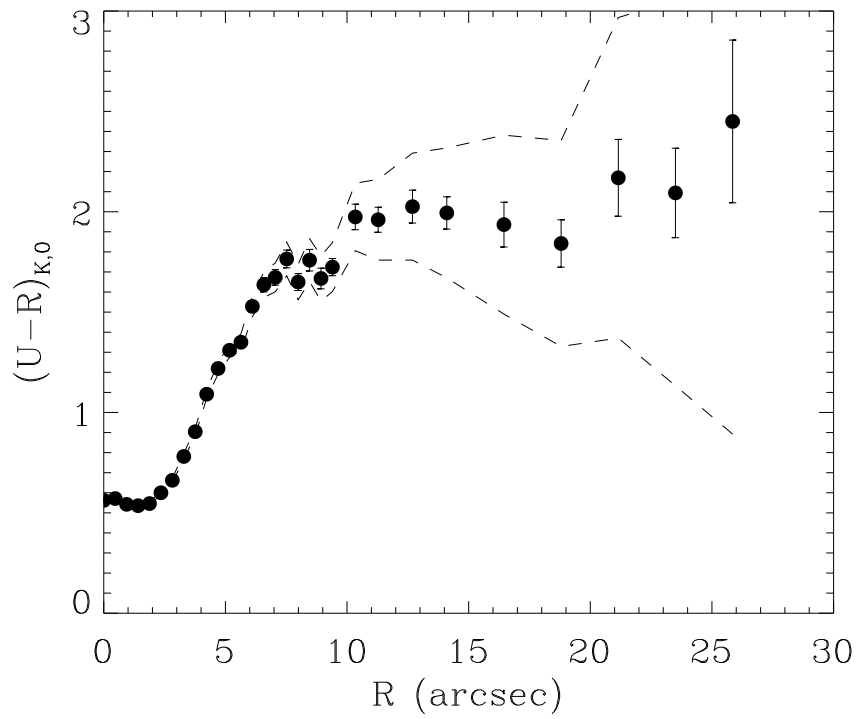


Fig. 3.— $U - R$ color profile of the cD showing the central blue colors associated with the starburst. Normal colors are $\sim 2.3 - 2.6$. The dashed lines represent the systematic uncertainty associated with sky background subtraction

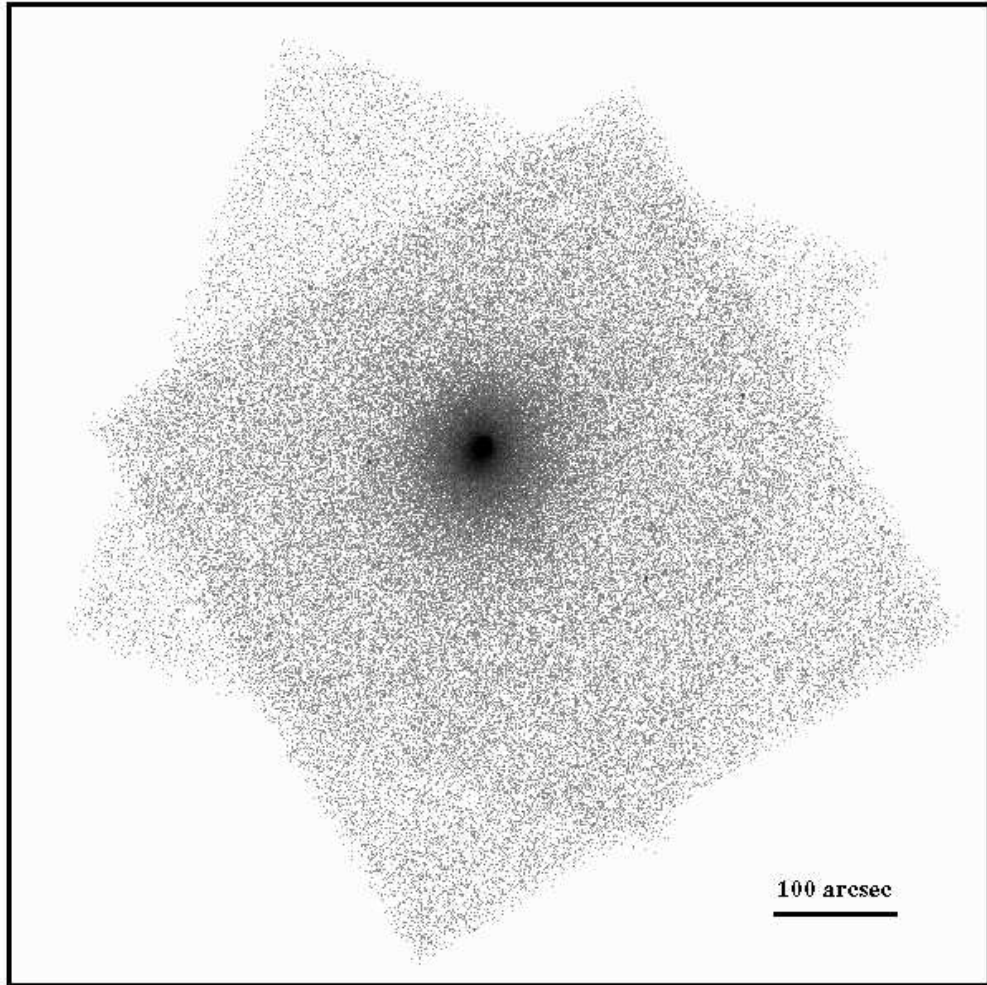


Fig. 4.— X-ray image of the cluster made with the combined 30-ks exposure.

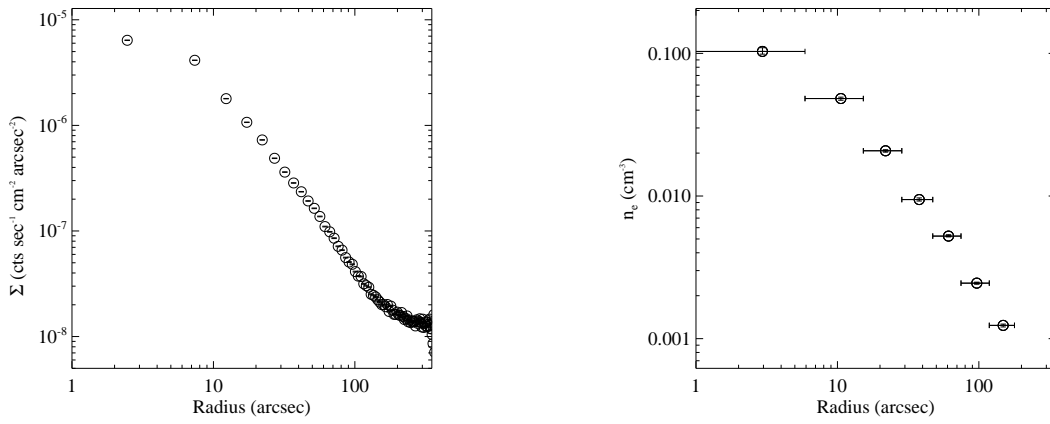


Fig. 5.— *Left:* X-ray surface brightness profile. *Right:* Density profile of the hot gas..

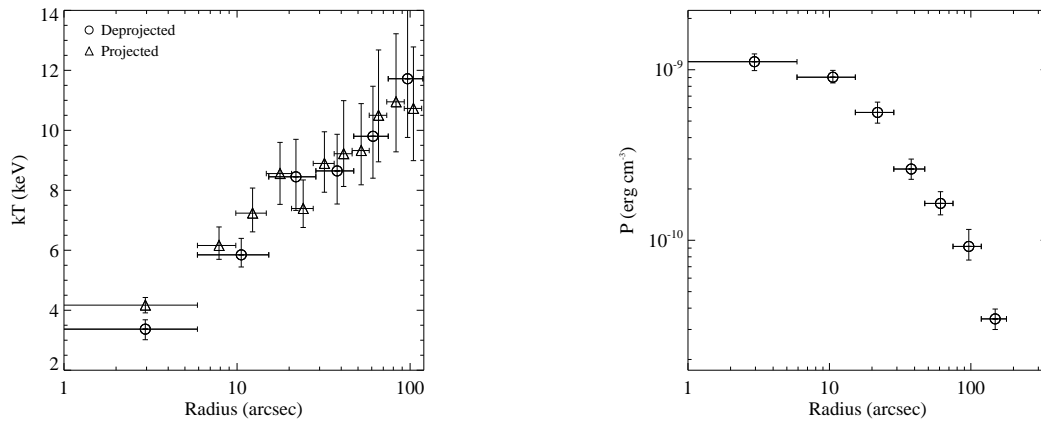


Fig. 6.— *Left*: Projected (triangles) and deprojected (circles) X-ray temperature profile of the hot gas. *Right*: Central pressure profile of the hot gas.

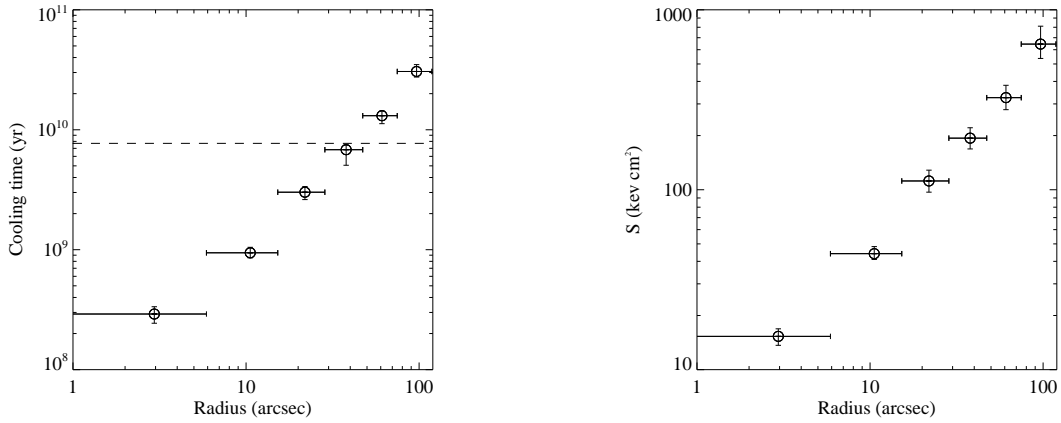


Fig. 7.— *Left*: Cooling time profile for the hot gas. The dashed line represents a cooling time of 7.7×10^9 yr, which is the look-back time to a redshift of one, which we assume to be roughly the epoch of cluster formation. This corresponds to a cooling radius of 41 arcsec or 161 kpc. *Right*: Entropy profile of the hot gas.

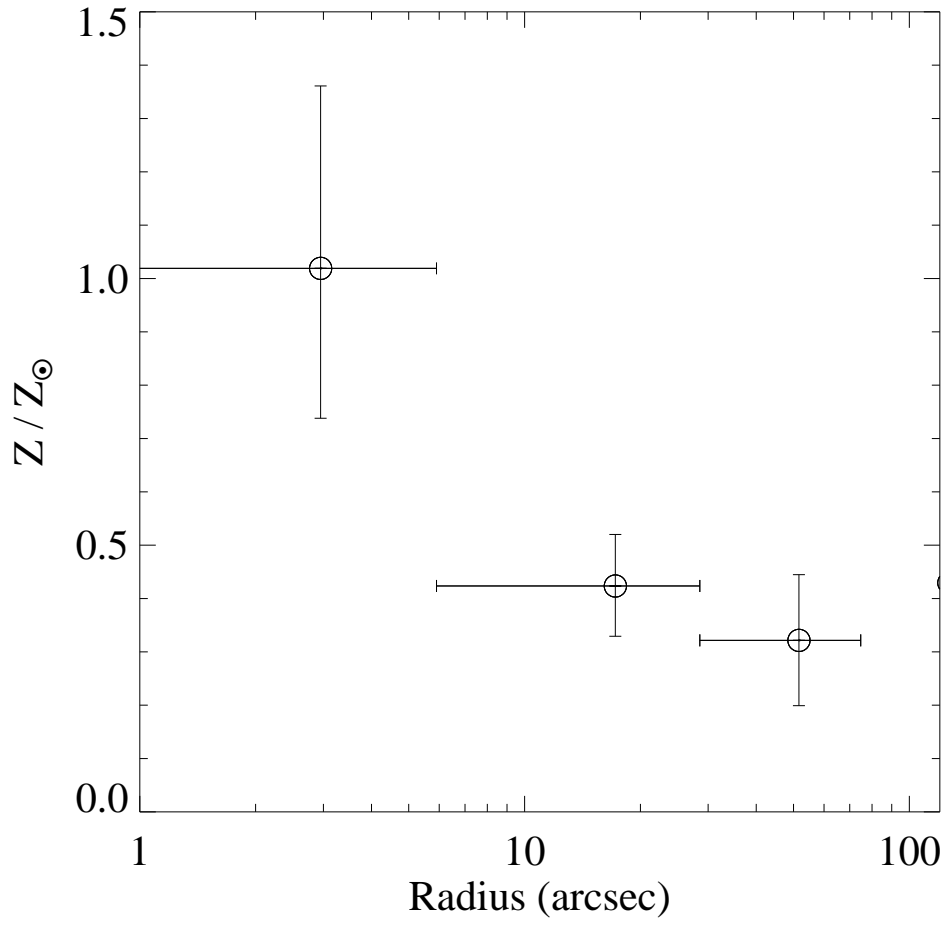


Fig. 8.— Abundance profile of the hot gas in solar units.

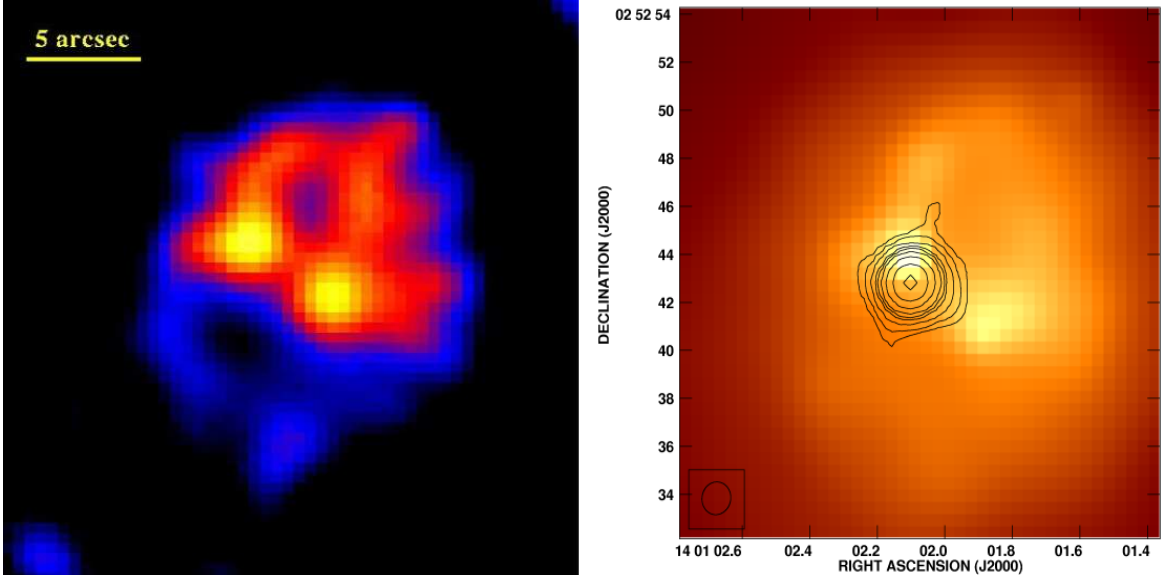


Fig.9 – *left*: 66.5 ksec image of the core of the cluster taken recently with the ACIS-I detector (Wise et al. 2006, private communication) showing the pair of cavities to the north west and south east of the nucleus, which lies between the bright spots of emission near the center of the picture. *Right*: Shorter ACIS-S X-ray image on which the X-ray analysis was done showing the radio source superposed.

Table 1. Starburst Properties

Cluster	SFR	M_{gas}	R_{burst}	$\log \Sigma_{\text{SFR}}$	$\log \Sigma_{\text{gas}}$	$\tau_{\text{dyn}}^{\text{a}}$	$\log \Sigma_{\text{gas}} / \tau_{\text{dyn}}$
...	$M_{\odot} \text{ yr}^{-1}$	M_{\odot}	kpc	$M_{\odot} \text{ yr}^{-1} \text{ kpc}^{-2}$	$M_{\odot} \text{ pc}^{-2}$	yr	$M_{\odot} \text{ yr}^{-1} \text{ pc}^{-2}$
Abell 1835	100 – 180	9×10^{10}	30	–1.19	1.51	6.6×10^8	2.14 ^a
Abell 1068	20 – 70	4×10^{10}	10	–0.65	2.12	2.2×10^8	2.25 ^a

^aassumes a stellar velocity dispersion of 281 km s^{-1} (Bîrzan et al. 2004)

Table 2. Cavity Properties

Cavity ...	R kpc	a kpc	b kpc	p 10^{-9} erg cm^{-3}	kT keV	pV 10^{59} erg	t Myr
North-west	23.3	15.5	11.6	1.0 ± 0.1	4.3 ± 0.4	$2.6^{+2.9}_{-1.0}$	41
South-east	16.6	13.6	9.7	1.1 ± 0.1	3.8 ± 0.3	$1.7^{+1.8}_{-0.3}$	27